

Pseudoscalar mesons with symmetric bound state vertex functions on the light front

George H. S. Yabusaki,^{1,*} Ishtiaq Ahmed,^{1,2,†} M. Ali Paracha,^{3,‡} J. P. B. C. de Melo,^{1,§} and Bruno El-Bennich^{1,4,¶}

¹*Laboratório de Física Teórica e Computacional,*

Universidade Cruzeiro do Sul, 01506-000, São Paulo, SP, Brasil

²*National Centre for Physics, Quaid-i-Azam University Campus, Islamabad, 45320 Pakistan*

³*Department of Physics, School of Natural Sciences,*

National University of Science and Technology, Islamabad, Pakistan

⁴*Instituto de Física Teórica, Universidade Estadual Paulista, 01140-070 São Paulo, SP, Brazil*

(Dated: June 19, 2021)

We study the electromagnetic form factors, decay constants and charge radii of the pion and kaon within the framework of light-front field theory formalism where we use an ansatz for the quark-meson interaction bound-state function which is symmetric under exchange of quark and antiquark momentum. The above mentioned observables are evaluated for the + component of the electromagnetic current, J^+ , in the Breit frame. We also check the invariance of these observables in other frames, whereby both the valence and the non-valence contributions have to be taken into account, and study the sensitivity of the electromagnetic form factors and charge radius to the model's parameters; namely, the quark masses, $m_u = m_d$, m_s , and the regulator mass, m_R . It is found that after a fine tuning of the regulator mass, i.e. $m_R = 0.6$ GeV, the model is suitable to fit the available experimental data within the theoretical uncertainties of both the pion and kaon.

PACS numbers:

I. INTRODUCTION

The theory of strong interactions, Quantum Chromodynamics (QCD), has been the object of theoretical and experimental scrutiny for four decades now and is perturbatively well defined. Indeed, at large momentum transfer, perturbative calculations successfully describe a wealth of subatomic phenomena. However, QCD is also a theory whose elementary excitations are confined and even in the far infrared below the typical hadronic scale, $E \approx 1$ GeV, QCD does not seem to break down [1–3]. Thus, nonperturbatively QCD may well be rigorously defined but a full solution is yet out of reach: there exists no simple Schrödinger picture of a many-body Hamiltonian as in quantum mechanics [4]. This is due to the intrinsic nonperturbative nature of quark-antiquark pair creation and annihilation in a relativistic quantum field theory, which entails non-conservation of particle number. In hadron physics, this situation leads to seek computational approaches beyond perturbative QCD and many models or effective theories have been proposed to tackle QCD in the nonperturbative regime with the aim to describe hadron phenomenology.

In this context, one possibility to develop a nonperturbative covariant framework is the light-front field theory formalism proposed by Dirac in 1949 [5]. In this approach, the hadronic bound states are described by wave functions in the light-front space-time hyper surface, de-

finied by the coordinate $x^+ = x^0 + x^3 = 0$, and due to the stability of the Fock-state decomposition these wave functions are covariant under kinematic boosts [4, 6].

On the other hand, in understanding the dynamical properties of nonperturbative QCD, the light pseudoscalar mesons and in particular the pion play a crucial role. Remarkably, the latter is a bound state of massive antiquark-quark pairs as well as the almost massless Goldstone boson associated with chiral symmetry breaking. There have been many studies of their static properties [7–12] and their dynamical properties have also been investigated theoretically [13–17, 24–62] and experimentally [64–74].

Taking advantage of the simple structure of the Fock space and the vacuum in light-front quantization, various hadronic properties of bound states, such as decay constants and electromagnetic form factors of the pion, kaon and nucleon, have been calculated [16, 17, 52–62] and successfully compared with their experimental values [64–74]. Since the light front component, J^+ , has been successfully employed to calculate electromagnetic form factors [7, 31, 63, 75–79], the light-front approach also offers a theoretical framework to extract from them useful information on the valence and non-valence components of the meson's wave function.

In the present simultaneous study of electromagnetic form factors, charge radii and decay constants, we adopt the light-front field theory formalism of Refs. [7, 15] wherein the Bethe-Salpeter amplitude of the $q\bar{q}$ bound states was modeled for two different momentum constellations, namely a symmetric [17] and nonsymmetric vertex model [16]. Here, the vertex refers to the $\bar{q}q$ pair coupling to the pseudoscalar meson in an effective Lagrangian. Using a nonsymmetric vertex model, E. O. Silva *et. al.* [58] calculated the aforementioned

*Electronic address: yabusaki@gmail.com

†Electronic address: ishtiaq@ncp.edu.pk

‡Electronic address: aliphoton9@gmail.com

§Electronic address: joao.mello@cruzeirodosul.edu.br

¶Electronic address: bruno.bennich@cruzeirodosul.edu.br

pion and kaon observables which are in agreement with experimental data. However, a momentum distribution of the meson that is symmetric under the exchange of the quark and antiquark momenta is more realistic and such a model for the Bethe-Salpeter amplitude should improve the description of or at least equally well reproduce all observables presented in Ref. [58]. Thus, we here use the same component, J^+ , of the light-front electromagnetic current, though with a symmetric momentum description of quark-meson bound-state vertex. It is important to recall here that the choice of J^+ with the Drell-Yan condition $q^+ = 0$ guarantees that pair-term contributions (non-valence terms) vanish [16, 17]. On the other hand, to preserve rotational symmetry, the pair contribution must be included [18–23]. Consequently, we here employ both the valence and non-valence contributions considering the case $q^+ \neq 0$.

This paper is organized as follows: Sec. II serves to summarize the general framework where subsequently the different physical observables, namely the electromagnetic form factors, decay constant and charge radii are discussed in turn. In Sec. III, we present our numerical results and analyze the observables' dependence on variation of the model parameters. In the last section, we give our conclusions.

II. THE MODEL

In this section, we briefly summarize the model and the computational tools of the light-front formalism required to investigate the pseudoscalar meson's electromagnetic form factors, charge radii and the decay constants. Our approach is based on similar earlier work [16, 17], where the following effective Lagrangian for the $\bar{q}q$ bound state was employed:

$$\mathcal{L}_{\text{eff}} = -ig\vec{\phi} \cdot \bar{q}\gamma^5\vec{\tau}q, \quad (1)$$

where $g = m_{0^-}/f_{0^-}$ is the coupling constant, m_{0^-} and f_{0^-} denote the mass and decay constant of a pseudoscalar meson, respectively, and $\vec{\phi}$ represents the scalar field. We make a symmetric ansatz for the $\bar{q}q$ -meson vertex which describes the bound state,

$$\Lambda(k, P) = \mathcal{C}[(k^2 - m_R^2 + i\epsilon)^{-1} + ((P - k)^2 - m_R^2 + i\epsilon)^{-1}], \quad (2)$$

where it is clear that the $\Lambda(k, P)$ is symmetric under the exchange of the quark and antiquark momenta, k and $(P - k)$; P is the total momentum of the meson and \mathcal{C} a normalization constant. In the following, we discuss the analytic light-front formulation of the electromagnetic form factor, charge radius and decay constant.

A. Electromagnetic form factors

The covariant electromagnetic form factor, $F_{0^-}^{\text{em}}$ is defined by a matrix element where the electromagnetic cur-

rent, $J_\mu = e_q\bar{q}\gamma_\mu q$, is sandwiched between the initial and final bound states of the same meson:

$$P_\mu F_{0^-}^{\text{em}}(q^2) = \langle M_{0^-}(p') | J_\mu | M_{0^-}(p) \rangle, \quad (3)$$

where $M_{0^-} = \pi^+, K^+$, $P_\mu = (p + p')_\mu$ and $q^2 = (p - p')^2$ is the square of the momentum transfer.

The electromagnetic form factor in the impulse approximation is obtained from triangle diagrams, each of which contains one spectator quark. In this approximation, the covariant electromagnetic current of a pseudoscalar meson, J_μ , that enters Eq. (3) can be written as follows [80, 81]:

$$J_\mu = N \int \frac{d^4k}{(2\pi)^4} \text{Tr} \left[\frac{1}{\not{k} - m_{\bar{q}} + i\epsilon} \gamma^5 \frac{1}{\not{k} - \not{p}' - m_q + i\epsilon} \gamma^\mu \right. \\ \left. \times \frac{1}{\not{k} - \not{p} - m_q + i\epsilon} \gamma^5 \right] \Lambda(k, p') \Lambda(k, p) + [q \leftrightarrow \bar{q}], \quad (4)$$

with the normalization,

$$N = \frac{-2i e_q \hat{m}_{0^-}^2 N_c}{f_{0^-}^2}, \quad \hat{m}_{0^-} : \frac{m_q + m_{\bar{q}}}{2},$$

where $N_c = 3$ is the number of colors and f_{0^-} the pseudoscalar weak decay constant.

The light front-form variables are,

$$k^+ = k^0 + k^3, \quad k^- = k^0 - k^3, \quad \vec{k}_\perp \equiv (k^1, k^2) \\ q^+ = \sqrt{-q^2} \sin \alpha, \quad q_x = \sqrt{-q^2} \cos \alpha, \quad q_y = 0 \\ q^2 = q^+ q^- - (\vec{q}_\perp)^2. \quad (5)$$

Here, we use the Drell-Yan condition, $q^+ = 0$, in the Breit frame, which implies $\alpha = 0$. However, our results are frame invariant, i.e. invariant for $\alpha \neq 0$ where both the valence and the non-valence contributions become important. After introducing the front-form variables in Eq. (5) and using $\gamma^+ = \gamma^0 + \gamma^3$ to obtain the J^+ component of the current in Eq. (4), the electromagnetic form factor becomes:

$$F_{X^{0^-}}^{\text{em}}(q^2) = \frac{N}{P^+} \int \frac{d^2k_\perp}{(2\pi)^4} dk^+ dk^- \text{Tr} [\mathcal{O}^+] \\ \times \Gamma(k^+, p^+, p'^+) + [q \leftrightarrow \bar{q}], \quad (6)$$

In Eq. (6), the trace in light-front coordinates is,

$$\frac{1}{4} \text{Tr}[\mathcal{O}^+] = \frac{1}{4} k^+ q_\perp^2 + (k^+ - p^+ - p'^+)(k_\perp^2 - k^+ k^-) \\ - k^- p^+ p'^+ - (p'^+ k_\perp \cdot p_\perp + p^+ k_\perp \cdot p'_\perp) \\ - k^+ (2k_\perp^2 + m_{\bar{q}}^2 - 2m_q m_{\bar{q}}) - (p^+ + p'^+) m_q m_{\bar{q}}, \quad (7)$$

and

$$\Gamma(k^+, p^+, p'^+) = \frac{\Lambda(k^+, p^+) \Lambda(k^+, p'^+)}{(k^2 - m_{\bar{q}}^2 + i\epsilon)((p - k)^2 - m_q^2 + i\epsilon)} \\ \times \frac{1}{((p' - k)^2 - m_q^2 + i\epsilon)}, \quad (8)$$

where $k^2 = k^+(k^- - k_{\text{on}}^-)$ where k_{on}^- is the on-energy-shell value of the corresponding momentum given by,

$$k_{\text{on}}^- = \frac{k_{\perp}^2 + m_{\bar{q}}^2}{k^+}. \quad (9)$$

In terms of light-front variables, the bound-state function in Eq. (2) becomes,

$$\begin{aligned} \Lambda(k^+, p^+) &= \frac{\mathcal{C}}{(p^+ - k^+)(p^- - k^- - \frac{(p-k)_{\perp}^2 + m_R^2 - i\epsilon}{p^+ - k^+})} \\ &+ \frac{\mathcal{C}}{k^+(k^- - \frac{k_{\perp}^2 + m_R^2 - i\epsilon}{k^+})}. \end{aligned} \quad (10)$$

Collecting all ingredients from Eqs. (7)–(10), we insert them in Eq. (6) and after k^- energy integration (see appendix of Ref. [17]) with $x = \frac{k^+}{p^+}$ the electromagnetic form factor can be rewritten,

$$\begin{aligned} F_{0^-}^{\text{em}} &= \frac{\mathcal{N}}{P^+} \int \frac{d^2 k_{\perp} dx}{x(1-x)} \Phi^*(x, k_{\perp}) \Phi(x, k_{\perp}) \theta(x) \theta(1-x) \\ &\times \left[\frac{1}{4} k^+ q_{\perp}^2 - k_{\text{on}}^- p^+ p'^+ - (p'^+ k_{\perp} \cdot p_{\perp} + p^+ k_{\perp} \cdot p'_{\perp}) \right] \end{aligned} \quad (11)$$

where $\mathcal{N} = \frac{N_c^2}{(2\pi)^3}$ and

$$\begin{aligned} \Phi(x, k_{\perp}, p^+, \vec{p}_{\perp}) &= \left[\frac{1}{(1-x)(m_{0^-}^2 - \mathcal{M}^2(m_q^2, m_R^2))} \right. \\ &+ \left. \frac{1}{x(m_{0^-}^2 - \mathcal{M}^2(m_R^2, m_q^2))} \right] \frac{1}{m_{0^-}^2 - \mathcal{M}^2(m_q^2, m_q^2)}, \\ &+ [q \leftrightarrow \bar{q}] \end{aligned} \quad (12)$$

with

$$\mathcal{M}^2(m_a^2, m_b^2) = \frac{k_{\perp}^2 + m_a^2}{x} + \frac{(p-k)_{\perp}^2 + m_b^2}{(1-x)} - p_{\perp}^2$$

Note that the appearance of the second term of Eq. (12) is due to the symmetric character of the meson-quarks vertex, which is absent in Refs. [16, 58] where the authors consider a nonsymmetric behavior of the vertex function. As it was shown [16, 17, 25], to preserve general covariance the non-valence contribution is mandatory. Thus, in Eq. (11) the step functions $\theta(x)$ and $\theta(1-x)$ delimit the integration interval, $0 < k < p^+$, of the valence contribution, whereas the interval, $p^+ < k^+ < p'^+$, corresponds to the non-valence contributions to electromagnetic current [17].

B. Charge radius and decay constant

The mean-square electric charge radius of a meson is a relevant quantity and correlated with the electromagnetic form factor,

$$F_{0^-}^{\text{em}}(q^2) \simeq 1 - \frac{1}{6} \langle r_{0^-}^2 \rangle q^2. \quad (13)$$

Differentiation with respect to q^2 , of the above equation yields the charge radius,

$$\langle r_{0^-}^2 \rangle = \left. \frac{dF_{0^-}^{\text{em}}}{dq^2} \right|_{q^2=0}. \quad (14)$$

A relevant observable and also our main constraint on the model's parameters is given by the weak decay constant, f_{0^-} . The decay constant of a $q\bar{q}$, bound state can be found from the following matrix element of the partially conserved axial-vector current:

$$\langle 0 | A^{\mu} | 0^- \rangle = i f_{0^-} p^{\mu}. \quad (15)$$

where $A^{\mu} = \bar{q} \gamma^{\mu} \gamma^5 q$, is the axialvector current. The weak decay constant is given by,

$$\begin{aligned} f_{0^-} &= \frac{i N_c}{f_{0^-}} \int \frac{d^4 k}{(2\pi)^4} \text{Tr} \left[\not{p} \gamma^5 \frac{\not{k}}{k^2 - m_q^2 + i\epsilon} \right. \\ &+ \left. \gamma^5 \frac{(\not{k} - \not{p})}{(k-p)^2 - m_{\bar{q}}^2 + i\epsilon} \right] \Lambda(k, p) \end{aligned} \quad (16)$$

We make use of the + component of the axialvector current A^+ and after integration over k^- , one obtains the decay constant in terms of the valence component of the model:

$$f_{0^-} = \frac{\sqrt{N_c}}{4\pi^3} \int \frac{d^2 k_{\perp} dx}{x} [4x m_q + 4m_q(1-x)] \Phi(x, k_{\perp}, m_{\pi}, \vec{0}). \quad (17)$$

III. NUMERICAL RESULTS AND DISCUSSION

The model introduced in Sec. II contains three free parameters, namely, the regulator mass, m_R , and the two constituent quark masses, $m_u = m_d$ and $m_{\bar{s}}$, where the strange quark mass is taken from the study in Ref. [24]. The main focus of this study is to constrain the parameters of a more realistic bound-state ansatz to accommodate the available experimental data on the pion and kaon elastic form factors, decay constants and charge radii. In addition, it is also instructive and important to check the explicit dependence of these observables on the model's parameter.

Regarding these goals, we know from a previous study [17] that the value of the regulator mass, $m_R = 0.6$ GeV, reproduces well all experimental data on the pion observables mentioned above. It is worthwhile to check whether $m_R = 0.6$ GeV is also consistent with the kaon data, for which we compute the values of the decay constants and charge radii and compare them with their experimental values.

The calculated values of the observables listed in Table I show that $m_R = 0.6$ GeV is also a suitable value for the kaon. Moreover, for $m_{\bar{s}} = 0.44$ GeV,

Decay Constant and Charge radius	$m_R = 0.6 \text{ GeV}; m_{\bar{s}} = 0.44 \text{ GeV}$			
	Pion		Kaon	
	$m_u = m_d = 0.22 \text{ GeV}$	$m_u = m_d = 0.25 \text{ GeV}$	$m_u = m_d = 0.22 \text{ GeV}$	$m_u = m_d = 0.25 \text{ GeV}$
f_{0^-}	93.12 MeV	101.85 MeV	110.81 MeV	113.74 MeV
$\langle r_{0^-} \rangle$	0.736 fm	0.670 fm	0.754 fm	0.687 fm

TABLE I: Calculated decay constants and charge radius for two light-quark masses and corresponding experimental values. The experimental date with errors bar, are; $f_{\pi}^{\text{exp}} = 92.42 \pm 0.021 \text{ MeV}$, $\langle r_{\pi} \rangle^{\text{exp}} = 0.672 \pm 0.008 \text{ fm}$, $f_K^{\text{exp}} = 110.38 \pm 0.1413$ and $\langle r_K \rangle^{\text{exp}} = 0.560 \pm 0.031 \text{ fm}$. Experimental date from [64, 70, 82].

$m_u = m_d = 0.22 \text{ GeV}$ and $m_R = 0.6 \text{ GeV}$, the deviation from the experimental values of f_{π^+} (f_{K^+}) and $\langle r_{\pi^+} \rangle$ ($\langle r_{K^+} \rangle$) are 0.76% (0.37%) and 8.7% (34.10%), while with $m_u = m_d = 0.25 \text{ GeV}$, the mismatch is 9.3% (3.02%) and 0.35% (22.68%), respectively.

For comparison, we recall that in case of a non-symmetric vertex function the ratio of decay constants, f_K/f_{π} , which measures $SU(3)$ flavor-symmetry breaking, was found to be 1.363 [58]. Here, we read from the table that $f_K/f_{\pi} \simeq 1.189$, which is closer to the measured value i.e., $f_K^{\text{exp}}/f_{\pi}^{\text{exp}} = 1.197 \pm 0.002 \pm 0.006$ [82]. A graphic representation of the explicit dependence of the form factors, F_0^{em} , decay constants, f_{0^-} and charge radii $\langle r_{0^-} \rangle$ on the model's parameters can be found in Figs. 1 to 8, in each of which one parameter is fixed while the other is varied.

In Figs. 1 and 2, we plot the electromagnetic form factors of the pion and kaon as a function of q^2 for various values of m_R and $m_u = m_d$ and $m_{\bar{s}}$ fixed. As can be

seen, the elastic form factors in both figures are monotonically decreasing functions of q^2 with increasing hardness for larger values of m_R . Fig. 1 also informs us that the available experimental pion data lie in the interval of $0.1 \text{ GeV} \leq m_R \leq 1 \text{ GeV}$ and from Fig. 2 we deduce that the kaon's experimental form factor data are better reproduced for $m_R \gtrsim 0.5 \text{ GeV}$ which coincides with our privileged value, $m_R = 0.6 \text{ GeV}$.

Similarly, in Figs. 3 and 4, the electromagnetic form factors of the pion and kaon are plotted as a function of q^2 for different values of $m_u = m_d$ whereas $m_R = 0.6 \text{ GeV}$ is fixed. One observes a likewise behavior of the electromagnetic form factors, i.e. $F^{\text{em}}(q^2)$ becomes harder for increasing values of $m_u = m_d$. We note that for the symmetric vertex function with $m_R = 0.6 \text{ GeV}$, the light-quark mass should be in the range $0.15 \lesssim m_q \lesssim 0.5 \text{ GeV}$, where the constituent quark mass, $m_q = 0.22 \text{ GeV}$, appears to be the most favorable value to accommodate the experimental data.

Next, the explicit dependence of the charge radii $\langle r_{\pi} \rangle$

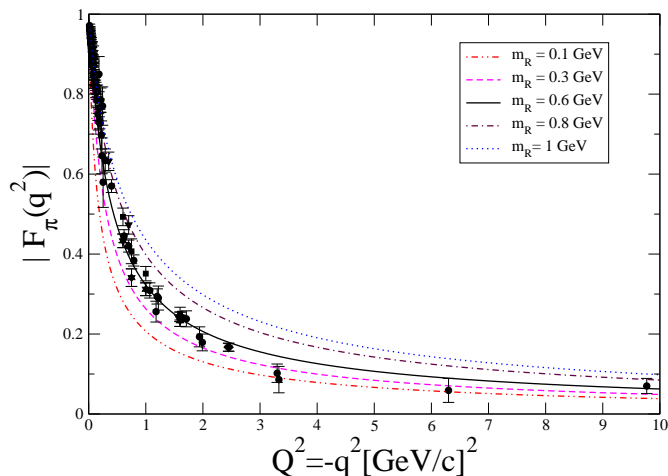


FIG. 1: The electromagnetic form factor of the pion as a function of space-like q^2 . The curves correspond to the different values of m_R with fixed quark masses: $m_u = m_d = 0.220 \text{ GeV}$. Experimental data: Ref. [66] (circle), Ref. [65] (square), Ref. [68] (diamonds), Ref. [69] (up triangle), Ref. [73] (down triangle).

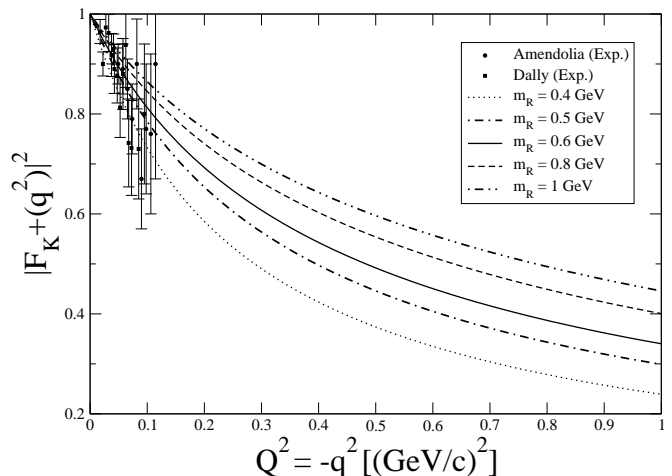


FIG. 2: The electromagnetic form factor of the kaon as a function of space-like q^2 . The curves correspond to the different values of m_R with fixed quark masses: $m_u = m_d = 0.220 \text{ GeV}$, $m_{\bar{s}} = 0.44 \text{ GeV}$. Experimental data: Ref. [83] (square), Ref. [64] (circle).

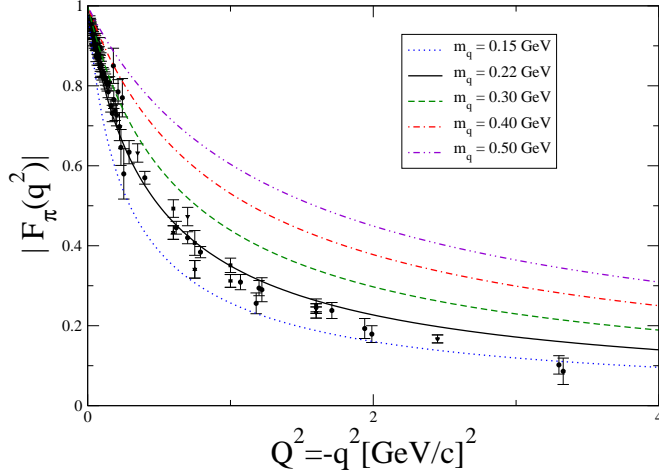


FIG. 3: The electromagnetic form factor of the pion as a function of space-like q^2 . The curves correspond to different values of $m_q = m_u$ with regulator mass $m_R = 0.60$ GeV. Experimental data: Ref. [66] (circle), Ref. [65] (square), Ref. [68] (diamonds), Ref. [69] (up triangle), Ref. [73] (down triangle).

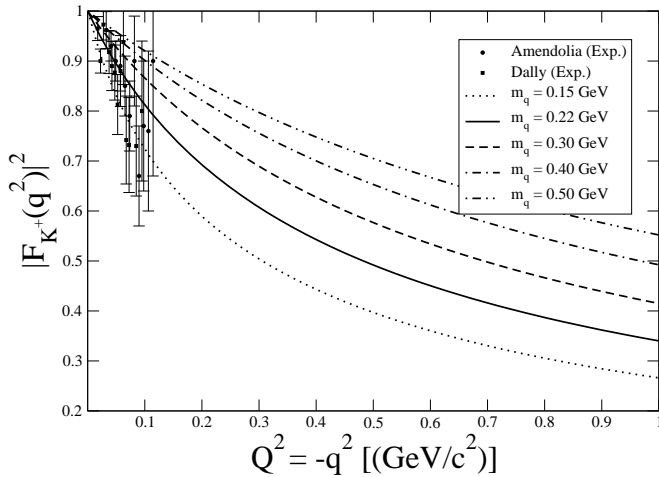


FIG. 4: The electromagnetic form factor of the kaon as a function of space-like q^2 . The curves correspond to different values of $m_q = m_u$ with fixed masses: $m_{\bar{s}} = 0.44$ GeV, $m_R = 0.60$ GeV. Experimental data: solid circle [64] (circle) and square [83].

and $\langle r_K \rangle$ on $m_u = m_d$ is depicted in Fig. 5 from which we deduce that the charge radius exhibits a nonlinear behavior and decreases strongly for large values of $m_u = m_d$, as expected. For instance, for $m_u = m_d = 0.15$ GeV, the size of the pion (kaon) charge radius is about 0.98 fm (~ 1 fm), whereas for $m_u = m_d = 0.5$ GeV this size reduces to 0.43 fm (0.45 fm). A similar behavior can

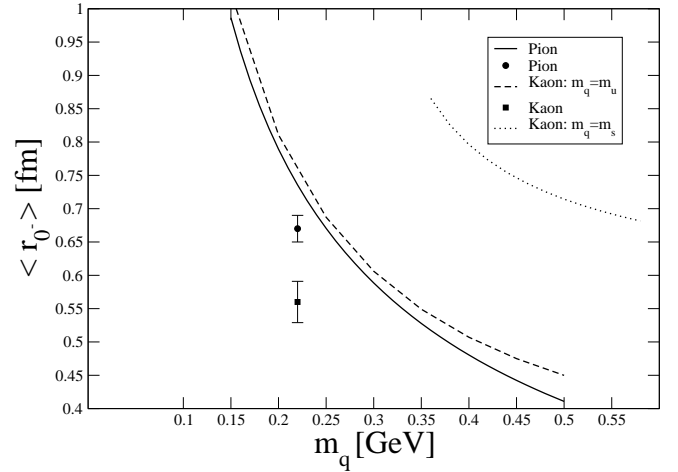


FIG. 5: Charge radii $\langle r_{0-} \rangle$ of the pion and kaon as a function of the constituent quark mass $m_u = m_d$ with $m_{\bar{s}} = 0.44$ GeV and fixed regulator mass $m_R = 0.6$ GeV. The solid circle [70] and square [64] are the experimental values for the charge radii of the pion and kaon, respectively.

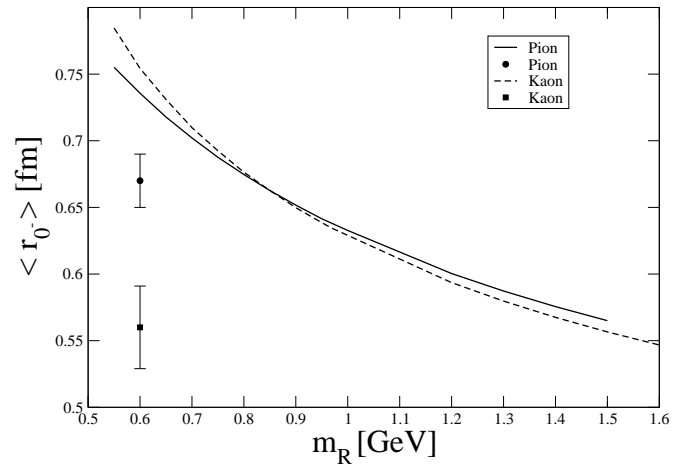


FIG. 6: Charge radii $\langle r_{0-} \rangle$ of the pion and kaon as a function of the regulator mass m_R with $m_u = m_d = 0.22$ GeV and $m_{\bar{s}} = 0.44$ GeV fixed. The solid circle [70] and the square [64] are the experimental charge radii values of the pion and kaon, respectively.

be seen in Fig. 6, where the charge radii are plotted against the regulator mass m_R with $m_u = m_d = 0.22$ GeV and $m_{\bar{s}} = 0.44$ GeV. However, these effects are less pronounced for variations of m_R than of $m_u = m_d$.

Finally, the weak decay constants, f_π and f_K , are plotted in Fig. 7 and Fig. 8 as functions of $m_u = m_d$

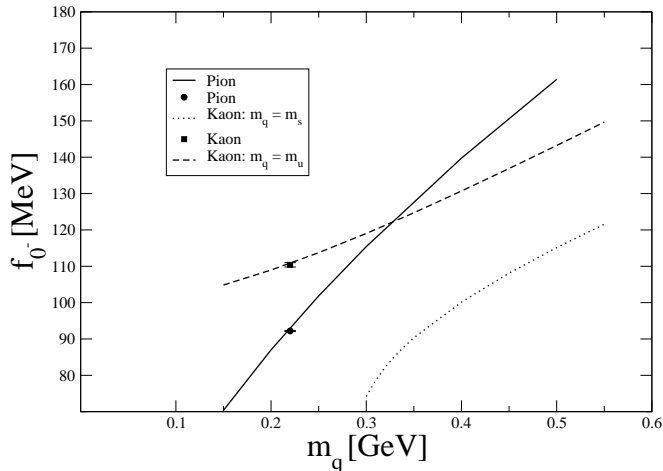


FIG. 7: The weak decay constants f_{0-} of the pion (solid curve with $m_u = m_d = 0.22$ GeV) and kaon (dashed curve: $m_{\bar{s}} = 0.44$ GeV) as a function of $m_u = m_d$; dotted curve: kaon decay constant as a function of $m_{\bar{s}}$. In all curves $m_R = 0.6$ GeV. The solid circle and square are the experimental decay constants of the pion and kaon, respectively [82].

($m_R = 0.6$ GeV) and m_R ($m_u = m_d = 0.22$ GeV), where in both cases $m_{\bar{s}} = 0.44$ GeV. We observe that in contrast to the charge radii the decay constants are continuous increasing functions of m_q and m_R . Moreover, the charge radii and the decay constants are more sensitive to the quark mass values, m_q , than to m_R . It is worthwhile to point out, as discussed in Ref. [58] for the non-symmetric vertex, that the sensitivity of the kaon decay constant to the strange quark mass is very modest, whereas for the present symmetric vertex the $m_{\bar{s}}$ dependence is quite significant.

We stress that the regulator mass $m_R = 0.6$ yields the best fit to the experimental values of the decay constants and charge radii as discussed above. Furthermore, the decreasing (increasing) behavior of the charge radii (decay constants) with m_q , as depicted in Figs. 5 and 7, satisfies Tarrach's relation [84], i.e. $\langle r_{0-} \rangle \sim 1/m_q$ and $f_{0-} \sim 1/\langle r_{0-} \rangle$.

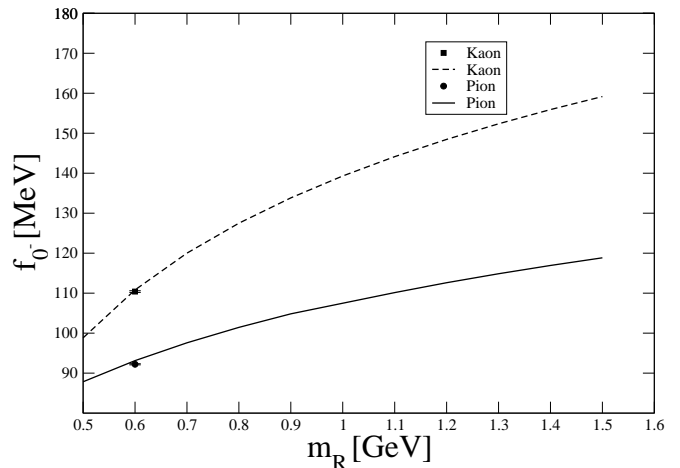


FIG. 8: The weak decay constant, f_{0-} , of the pion (solid curve) and kaon (dashed curve) as a function of the regulator mass m_R with $m_u = m_d = 0.22$ GeV and $m_{\bar{s}} = 0.44$ GeV fixed. The circles and the square are the experimental values or the charge radii of the pion and kaon, respectively [82].

IV. CONCLUSIONS

We reexamined the light-front approach to the light pseudoscalar mesons [16, 17, 58] by considering a symmetric $q\bar{q}$ bound-state function [17]. In this framework and with the given symmetric ansatz for the bound-state vertex function, we calculated the charge radii, $\langle r_{\pi} \rangle$, and $\langle r_K \rangle$, weak decay constants, f_{π} and f_K and the electric form factors, $F_{\pi}^{\text{em}}(q^2)$ and $F_K^{\text{em}}(q^2)$.

To constrain our model parameters, namely, the quark masses m_u , m_d and m_s and the regulator mass m_R , we first adjusted their values to reproduce the experimental weak decay constants. In doing so, we imposed the same regulator mass for both the pion and kaon and found that $m_R = 0.6$ GeV is a suitable value to describe all experimental data on $F_{\pi(K)}^{\text{em}}$, $\langle r_{\pi(K)} \rangle$ and $f_{\pi(K)}$ within the reasonable theoretical uncertainties. The numerical results also show this model significantly breaks down for $m_R \geq 1$ GeV, which was already demonstrated in the case of a nonsymmetric vertex function [58].

Moreover, the explicit dependence of charge radii and decay constants on the quark masses, $m_u = m_d$ and $m_{\bar{s}}$, not only satisfies Tarrach's relation but also favors the range of mass values commonly chosen within the light-front model. In addition, by using the privileged values of the model's parameters $m_u = m_d = 0.22$ GeV, $m_{\bar{s}} = 0.44$ GeV and $m_R = 0.6$ GeV, we find that the pion-to-kaon decay constant ratio is in excellent agreement with its experimental value, i.e. the mismatch is barely 0.67%. Lastly, the present numerical investigation suggests that these parameter values could also be used to study dynamical properties of other pseudoscalar and vector mesons or may apply to heavy-to-light transition form factors.

Acknowledgments

This work was supported by the Brazilian agencies FAPESP (Fundação de Amparo à Pesquisa do Estado de

São Paulo), CAPES (Coordenação de Aperfeiçoamento de Pessoal de Nível Superior and CNPq (Conselho Nacional de Desenvolvimento Científico e Tecnológico).

-
- [1] A. Bashir, L. Chang, I. C. Cloët, B. El-Bennich, Y. X. Liu, C. D. Roberts and P. C. Tandy, *Commun. Theor. Phys.* **58**, 79 (2012).
- [2] I. C. Cloët and C. D. Roberts, *Prog. Part. Nucl. Phys.* **77**, 1 (2014).
- [3] C. D. Roberts, arXiv:1501.06581 [nucl-th] (2015).
- [4] S. J. Brodsky, H.-C. Pauli, and S. S. Pinsky, *Phys. Rep.* **301**, 299 (1998).
- [5] P. A. M. Dirac, *Reviews of Modern Physics*, volume 21, 1949.
- [6] R. J. Perry, A. Harindranath, K. G. Wilson, *Phys. Rev. Lett.* **65**, 2959 (1990).
- [7] T. Frederico and G. Miller, *Phys. Rev. D* **45**, 4207 (1992).
- [8] P. Maris, C. D. Roberts and P. C. Tandy, *Phys. Lett. B* **420**, 267 (1998).
- [9] P. Maris and C. D. Roberts, *Phys. Rev. C* **56**, 3369 (1997).
- [10] P. Maris and P. C. Tandy, *Phys. Rev. C* **60**, 055214 (1999).
- [11] P. Maris and P. C. Tandy, *Phys. Rev. C* **61**, 045202 (2000).
- [12] D. Ebert, R. N. Faustov and V. O. Galkin, *Eur. Phys. J. C* **47**, 745 (2006).
- [13] G. P. Lepage and S. J. Brodsky, *Phys. Lett. B* **87**, 359 (1979).
- [14] G. P. Lepage and S. J. Brodsky, *Phys. Rev. D* **22**, 2157 (1980).
- [15] T. Frederico and G. A. Miller, *Phys. Rev. D* **50**, 210 (1994).
- [16] J. P. B. C. de Melo, H. W. L. Naus and T. Frederico, *Phys. Rev.* **C59**, 2278 (1999).
- [17] J. P. B. C. de Melo, T. Frederico, E. Pace and G. Salmè, *Nucl. Phys.* **A707**, 399 (2002); *Braz. J. Phys.* **33**, 301 (2003).
- [18] Bernard L. G. Bakker, Ho-Meoyng Choi and Chueng-Ryong Ji, *Phys. Rev. D* **63**, 074014 (2001).
- [19] A. Ioannian and J. W. F. Valle, *Phys. Rev. D* **63**, 073002 (2002).
- [20] Ho-Meoyng Choi and Chueng-Ryong Ji, *Phys. Rev. D* **70**, 053015 (2004).
- [21] Wolfgang Jaus, *Phys. Rev. D* **60**, 054026 (1999).
- [22] J. P. B. C. de Melo and T. Frederico, *Phys. Lett. B* **708**, 87 (2012).
- [23] F. Cardarelli et al., *Phys. Lett. B* 349 (1993) 393.
- [24] E. F. Suisso, J. P. B. C. de Melo and T. Frederico, *Phys. Rev. D* **65** 094009, (2002).
- [25] B. L. G. Bakker, H.-M. Choi, C.-R. Ji, *Phys. Rev. D* **63**, 074014 (2001).
- [26] P. Maris and P. C. Tandy, *Phys. Rev. C* **62**, 055204 (2000).
- [27] P. Maris and P. C. Tandy, *Phys. Rev. C* **65**, 045211 (2002).
- [28] H. L. L. Roberts, C. D. Roberts, A. Bashir, L. X. Gutiérrez-Guerrero and P. C. Tandy, *Phys. Rev. C* **82**, 065202 (2010).
- [29] Bertrand Desplanques, *Eur.Phys.J.* **A42**, 219 (2009).
- [30] T. Nguyen, A. Bashir, C. D. Roberts and P. C. Tandy, *Phys. Rev. C* **83**, 062201 (2011).
- [31] D. Melikhov and S. Simula, *Phys. Rev. D* **65**, 094043 (2002).
- [32] J. P. B. C. de Melo, T. Frederico, E. Pace and G. Salmè, *Phys. Lett. B* **581**, 75 (2004).
- [33] J. P. B. C. de Melo, T. Frederico, E. Pace, and G. Salmè, *Phys. Rev. D* **73**, 074013 (2006).
- [34] J. P. B. C. de Melo, J. S. Veiga, T. Frederico, E. Pace and G. Salmè, hep-ph/0609212.
- [35] Ho-Meoyng Choi and Chueng-Ryong Ji, *Phys. Rev. D* **75**, 034019 (2007).
- [36] Victor Braguta, Wolfgang Lucha and Dmitri Melikhov, *Phys. Lett. B* **661**, 354 (2008).
- [37] B. El-Bennich, J. P. B. C. de Melo, B. Loiseau, J.-P. Dondond and T. Frederico, *Braz. J. Phys.* **38**, 465 (2008).
- [38] B. El-Bennich and W. M. Kloet, *Phys. Rev. C* **70**, 034001 (2004).
- [39] B. El-Bennich and W. M. Kloet, *Phys. Rev. C* **70**, 034002 (2004).
- [40] B. El-Bennich, *Phys. Rev. C* **72**, 067001 (2005).
- [41] S. J. Brodsky and G. F. de Teramond, *Phys. Rev. D* **77**, 056007 (2008).
- [42] Cesareo A. Dominguez, Juan I. Jottar, Marcelo Loewe and Bernard Willers, *Phys. Rev. D* **76**, 09002 (2007).
- [43] Yu-bing Dong and Yizhan Wang, *J.Phys.* **G39**, 025003 (2012).
- [44] Udit Raha and Andreas Aste, *Phys. Rev.* **D79**, 034015 (2009).
- [45] Udit Raha, Hiroaki Kohyama, *Phys.Rev.* **D82**, 114012 (2010).
- [46] W. de Paula, T. Frederico, *Phys.Lett.* **B693**, 287 (2010).
- [47] Dylan Albrecht, Joshua Erlich, *Phys.Rev.* **D82**, 09500 (2010).
- [48] O. Leitner, J.-F. Mathiot and N. A. Tsirova, *Eur. Phys. J. A* **47**, 17 (2011).
- [49] H.-M. Choi and C.-R. Ji, *Phys. Rev. D* **59**, 034001 (1998).
- [50] Bernard L. G. Bakker and Chueng-Ryong Ji, *Prog. Part. Nucl. Phys.* **74**, 1 (2014).
- [51] Elmar P. Biernat, Franz Gross, Teresa Peña, Alfred Stadler, *Phys. Rev.* **D89**, 016006 (2014).
- [52] Hai-Yang Cheng, Chun-Khiang Chua and Chien-Wen Hwang, *Phys.Rev.* **D69**, 074025 (2004).
- [53] W. R. B. de Araujo, E. F. Suisso, T. Frederico, M. Beyer, H. J. Weber, *Phys. Lett.* **B478**, 86 (2000).
- [54] J. P. B. C. de Melo, T. Frederico, E. Pace and G. Salmè, *Phys. Lett.* **B581**, 75 (2004).
- [55] J. P. B. C. de Melo, T. Frederico, E. Pace and G. Salmè, *Phys. Rev.* **D73**, 074013 (2006).
- [56] J. P. B. C. de Melo, T. Frederico, E. Pace, S. Pisano and G. Salmè, *Phys. Lett. B* **671**, 153 (2009).
- [57] Fabiano Pereira, J. P. B. C. de Melo, T. Frederico and Lauro Tomio, *Nucl. Phys., A* **790**, 610 (2007).

- [58] Edson O. da Silva, J. P. B. C. de Melo, Bruno El-Bennich, and Victo S. Filho, Phys. Rev. **C86**, 038202 (2012).
- [59] Bruno El-Bennich, J. P. B. C. de Melo and Tobias Frederico, Few Body Syst. (2013).
- [60] J. P. B. C. de Melo, K. Tsushima, Bruno El-Bennich, E. Rojas and T. Frederico, Phys. Rev. **C 90**, 035201 (2014).
- [61] J. P. B. C. de Melo, B. El-Bennich and T. Frederico, Few Body Syst. (2014).
- [62] Jun He and Yu-bing Dong, J. Phys. **G32**, 189 (2006).
- [63] J. P. B. C. de Melo, T. Frederico, Phys. Rev. **C55**, 2043 (1997) 2043.
- [64] S. R. Amendolia *et al.*, Phys. Lett. B **178**, 435 (1986).
- [65] J. Volmer *et al.*, Phys. Rev. Lett. **86** 1713 (2001).
- [66] R. Baldini *et al.*, Eur. Phys. J. C **11** **709** (1999).
- [67] R. Baldini *et al.*, Nucl. Phys. A **666-667** 3 (2000).
- [68] T. Horn *et al.*, Phys. Rev. Lett. **97**, 192001 (2006).
- [69] V. Tadevosyan *et al.*, Phys Rev. C **75**, 055205 (2007).
- [70] S. R. Amendolia *et al.* [NA7 Collaboration], Nucl. Phys. B **277**, 168 (1986).
- [71] Brauel *et al.*, Phys. Lett. D **69**, 253 (1977).
- [72] T. Horn, X. Qian, J. Arrington, R. Asaturyan, F. Benmokhtar, W. Boeglin, P. Bosted and A. Bruell *et al.*, Phys. Rev. C **78**, 058201 (2008).
- [73] G. M. Huber *et al.* [Jefferson Lab Collaboration], Phys. Rev. C **78**, 045203 (2008).
- [74] H. P. Blok *et al.* [Jefferson Lab Collaboration], Phys. Rev. C **78**, 045202 (2008).
- [75] Z. Dziembowski and L. Mankiewicz, Phys. Rev. Lett. **58**, 2175 (1987).
- [76] F. Cardarelli, I. L. Grach, I. M. Narodetskii, G. Salmè, E. Pace and S. Simula, Phys. Rev. D **53**, 6682 (1996).
- [77] W. Jaus, Phys. Rev. D **60**, 054026 (1999).
- [78] H. Y. Cheng, C. K. Chua and C. W. Hwang, Phys. Rev. D **69**, 074025 (2004).
- [79] T. Huang and X. G. Wu, Phys. Rev. D **70**, 093013 (2004).
- [80] S. J. Brodsky, J. R. Primack, Ann. Phys. **52** (1969) 315, and references therein quoted.
- [81] F. Coester, D. O. Riska, Ann. Phys. **234**, 141 (1994).
- [82] K. A. Olive *et al.* (Particle Data Group), Chin. Phys. **C 38**, 090001 (2014).
- [83] E. B. Dally, J. M. Hauptman, J. Kubie, D. H. Stork, A. B. Watson, Z. Guzik, T. S. Nigmanov, V. D. Ryabstov *et al.*, Phys. Rev. Lett. **45**, 232 (1980).
- [84] R. Tarrach, Z. Phys. C **2**, 221 (1979).